

Vulcanization Characteristics and Dynamic Mechanical Behavior of Natural Rubber Reinforced with Silane Modified Silica

Wunpen Chonkaew¹, W. Mingvanish¹, U. Kungliean¹, N. Rochanawipart¹, and Witold Brostow^{2,*}

¹Department of Chemistry, Faculty of Science, King Mongkut's University of Technology Thonburi, Bangmod, Toongkru, Bangkok 10140, Thailand

²Laboratory of Advanced Polymers and Optimized Materials (LAPOM), Department of Materials Science and Engineering and Center for Advanced Research and Technology (CART), University of North Texas, 1150 Union Circle # 305310, TX 76203-5017, USA

Two silane coupling agents were used for hydrolysis-condensation reaction modification of nanosilica surfaces. The surface characteristics were analyzed using Fourier transform infrared spectroscopy (FTIR). The vulcanization kinetics of natural rubber (NR) + silica composites was studied and compared to behavior of the neat NR using differential scanning calorimetry (DSC) in the dynamic scan mode. Dynamic mechanical analysis (DMA) was performed to evaluate the effects of the surface modification. Activation energy E_a values for the reaction are obtained. The presence of silica, modified or otherwise, inhibits the vulcanization reaction of NR. The neat silica containing system has the lowest cure rate index and the highest activation energy for the vulcanization reaction. The coupling agent with longer chains causes more swelling and moves the glass transition temperature T_g downwards. Below the glass transition region, silica causes a lowering of the dynamic storage modulus G' , a result of hindering the cure reaction. Above the glass transition, silica—again modified or otherwise—provides the expected reinforcement effect.

Keywords: Nanocomposites, Natural Rubber Reinforcement, Dynamic Mechanical Analysis, Vulcanization.

1. INTRODUCTION

Natural rubber (NR) is extensively used in many applications due to its high elasticity (reversible deformability). However, the tensile modulus and strength of neat NR are low. For a number of applications, therefore, addition of a reinforcing phase is necessary.^{1–6} Silica is known as one of effective fillers for reinforcing rubber; it is primarily used in the production of light colored-products.⁶ Silica is used also to reinforce synthetic rubbers⁷ as well as epoxies.⁸ Vanadia is also used to strongly affect polymer properties,⁹ as are nanosized metals^{10–14} or carbon nanotubes.^{15–17}

Surfaces of silica, containing silanol and siloxane groups, are polar and hydrophilic. The hydrophilic character results in strong filler–filler interaction by hydrogen bonding—what leads to poor dispersion in rubber compounds.¹⁸ Moreover, the silanol groups are acidic and interact with the basic accelerators, causing detrimental

effects such as unacceptably long cure times and slow cure rates, and also lowering of crosslink density in sulphur-cured rubbers.^{19,20} To solve these problems, silane coupling agents such as bis(3-triethoxysilylpropyl) tetrasulphone (Si 69), bis(3-triethoxysilylpropyl) disulfide (TESPD), 3-thiocyanatopropyl triethoxysilane (Si-264) have been used.^{6,21–24} Silane coupling agents are primers for treating silica surfaces to make the filler compatible with rubber. Thus, Sae-oui et al.⁶ reported that Si 69 promoted the curing of NR containing silica particles and improved the dispersion of silica particles. There are at least two different ways to treat silica surface with a silane coupling agent. In the first approach, silica and silane are mixed together in a preliminary stage at optimized temperature and time. Alternatively, silane is added to the rubber together with silica, or else afterwards during mixing.

In this work, silica particles were pretreated with silane before mixing with natural rubber and curing. Two different types of silane, 3-methacryloxypropyl trimethoxysilane (MPTMS) and 3-mercaptopropyl trimethoxysilane

*Author to whom correspondence should be addressed.

(MPS), were used. The effects of these two silanes on curing behavior and also dynamic mechanical properties of NR + silica systems were investigated and compared with those of untreated and unreinforced systems.

2. EXPERIMENTAL DETAILS

2.1. Materials

Natural rubber (NR) used in this study was the Standard Thai 5L Rubber. It was purchased from Romphotiyoke, Thailand. Hydrophilic fumed silica with the average particle size of 12 nm (AEROSIL® 200) was purchased from Evonik Degussa, Thailand. 3-methacryloxypropyl trimethoxysilane (MPTMS) and 3-mercaptopropyl trimethoxysilane (MPS), used as silane coupling agents, were kindly supplied by Evonik Degussa, Thailand.

In addition to natural rubber, silica, and silanes, other additives used were zinc oxide, stearic acid, sulfur, tetramethyl thiuram monosulfide (TMTM), *N*-tert-butyl-2-benzothiazyl sulfonamide (TBBS) and poly(ethylene glycol) (PEG). All additives were commercial products used without further purification.

2.2. Preparation of Silane Treated Silica Particles

Modification of silica was carried out through hydrolysis and condensation. The amounts of silane added were kept constant at 10 wt% of silica. Silane hydrolysis was performed under acidic conditions by adding HCl into the

cosolvent of ethanol and water (95 wt% of ethanol) until obtaining pH \approx 2. After two hours of hydrolysis, the silane solution was added to the suspension of silica to perform the coupling reaction at the reflux temperature. The dried silica was first suspended in toluene. After the addition of silane solution, the mixture was refluxed for 5 hours and stirred further for 15 hours. The treated silica was recovered by evaporation method, rinsed and washed 3 times with toluene to remove the residual acid, and finally dried in an oven at 80 °C for 5 hours to obtain a constant weight. The hydrolysis and condensation reactions for preparing silane-treated silica particles are shown in Figure 1.

The Fourier transform infrared spectroscopy was carried out to confirm the successful coupling of silane on the surface of silica. A Perkin-Elmer 2000 FT-IR spectrometer was used.

2.3. Preparation of Rubber Compounds and Rubber Vulcanizates

Rubber compounds were prepared using a two-rolls mill. A vulcanization system used was of the conventional vulcanization (CV) type. Table I lists the compositions made.

Zinc oxide was incorporated into NR before the addition of silica, and then PEG, TMTM, TBBS, stearic acid, and finally sulfur were added to the composite.

Rubber vulcanizates were prepared by curing the rubber compounds in a hot-press at 140 °C based on the optimum cure time; see Section 2.4.

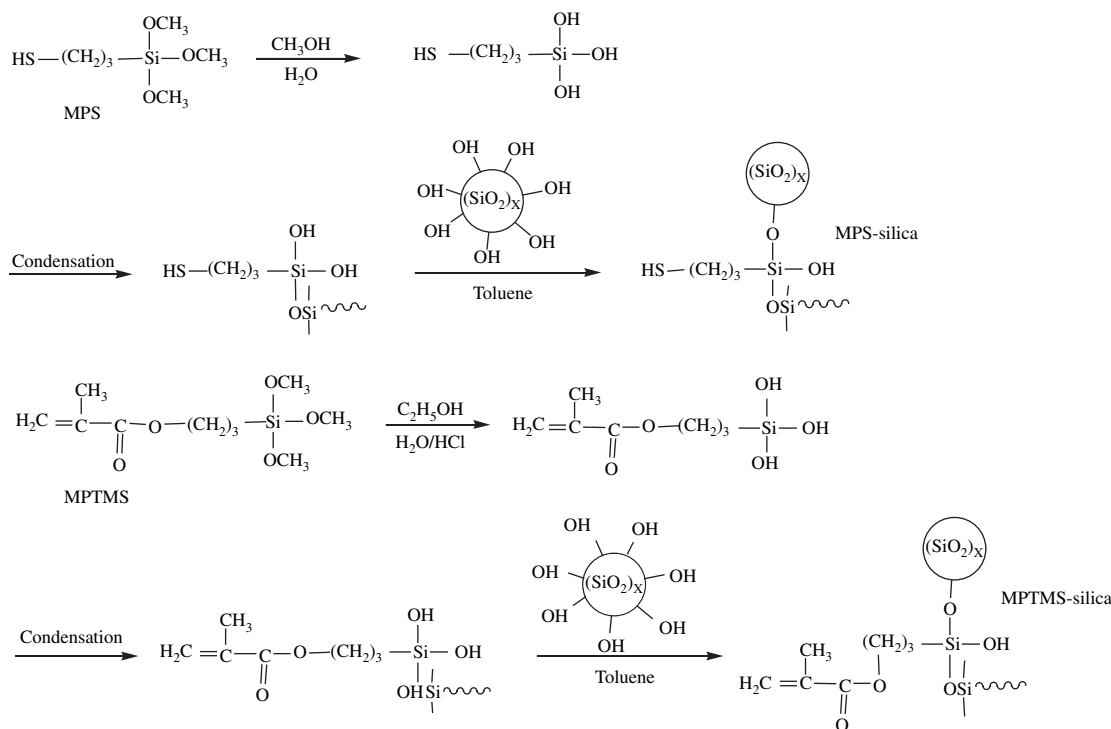


Fig. 1. Reaction scheme for preparing silane treated silicas: MPS-silica and MPTMS-silica.

Table I. Compositions of the nanohybrids.

Components	Neat NR (phr ^a)	Silica/NR (phr)	MPTMS-Silica/NR (phr)	MPS-Silica/NR (phr)
NR	100	100	100	100
Zinc oxide	5.0	5.0	5.0	5.0
Stearic acid	2.0	2.0	2.0	2.0
Sulfur	2.5	2.5	2.5	2.5
TMTM	1.0	1.0	1.0	1.0
TBBS	0.1	0.1	0.1	0.1
PEG	0.5	0.5	0.5	0.5
Nanosilica	—	20.0	—	—
MPTMS-silica	—	—	20.0	—
MPS-silica	—	—	—	20.0

^aParts per hundred parts of rubber.

2.4. Vulcanization Characteristics and Kinetics Studies

Curing characteristics of rubber compounds were determined using a Rubber Processing Analyzer (RPA2000, Alpha Technologies) at the temperature of 140 °C, the frequency of 1.67 Hz and the strain amplitude of 0.2°. The cure parameters such as the minimum torque (M_L), maximum torque (M_H), scorch time that represents the time for a rise by two units from minimum torque (t_{S2}), and cure time that corresponds to 90% of cure (t_{90}) and cure rate were investigated. The cure rate index (CRI) of the materials was calculated as

$$\text{CRI} = 100/(t_{90} - t_{S2}) \quad (1)$$

Reaction kinetics was determined using a power-compensated differential scanning calorimeter (DSC-7) of Perkin Elmer. The temperature and heat flow were calibrated with the melting temperature and heat of fusion of indium at each scanning rate applied. Nitrogen with the flow rate of 40 ml/min was used as the purge gas. Approximately 10 mg of each rubber compound was enclosed in an aluminum pan. The dynamic DSC method (temperature scan mode) was used to investigate the vulcanization kinetics.²⁵ The tests were run at 4 different scanning rates: 5, 10, 15 and 20 °C/min from 80 to 200 °C.

2.5. Dynamic Mechanical Analysis (DMA)

DMA was performed, using a Mettler Toledo DMA/SDTA861 apparatus in the shearing mode on strips of each rubber vulcanizate (5 mm of width × 5 mm of length × 2 mm of height). The temperature was scanned within the interval from -80 to +50 °C at 3 °C/min. The multi-frequency mode (1.0, 2.0, 5.0 and 10.0 Hz) was employed. To maintain the linear viscoelastic testing condition, the maximum force and amplitude applied on each sample were tested using the displacement scan method.

2.6. Swelling of Rubber Vulcanizates

The degree of swelling was determined according to ASTM D6814-02 and calculated²¹ as

$$Q\% = \frac{m_o - m}{m_o} \times 100 \quad (2)$$

where m_o and m were the weights of the sample before and after the swelling test, respectively. A 3 g sample of each rubber vulcanizate was immersed in toluene and kept in sealed containers for 72 hours; fresh solvent was replaced every 24-hours.

3. FTIR ANALYSIS

FTIR spectra of nanosilica and silane modified nanosilica were determined and are shown in Figure 2.

The broad hydrogen-bonded O–H stretching band at 3444 cm^{-1} is due to both water and SiOH groups while a peak at 1631 cm^{-1} is due to water. A strong absorption band between 1300 and 1000 cm^{-1} related to the asymmetry stretching of Si–O–Si bonds both in linear and cyclic forms is observed; the peak at 808 cm^{-1} is due to Si–OH. For silane modified nanosilicas (Fig. 2(b and c)), new peaks are found at 2857 and 2927 cm^{-1} ; they are attributed to the C–H stretching of CH_3 and CH_2 , respectively. These results indicate that some of the hydroxyl groups on the silica surface are substituted by organofunctional groups. Moreover, in the case of MPTMS treated nanosilica, the characteristic peak for $>\text{C}=\text{O}$ appears at 1701 cm^{-1} ; this confirms the presence of acrylate groups on the surface of silica.

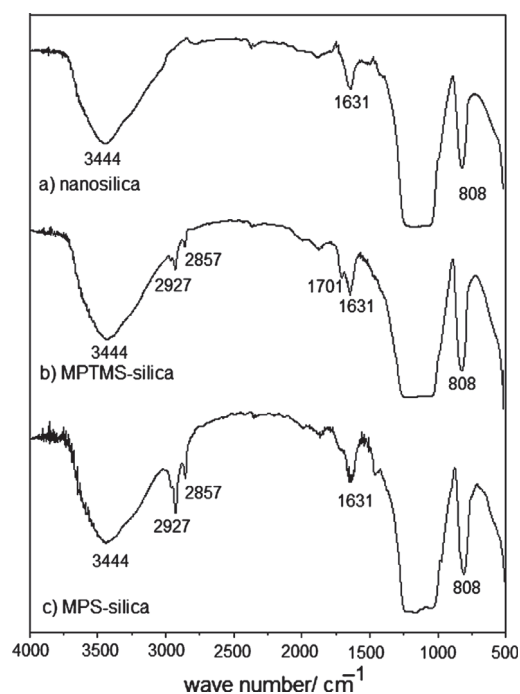
**Fig. 2.** FT-IR spectra of silicas.

Table II. The optimum cure time of the NR composites.

Samples	ΔS^a / (dN · m)	t_{S2} / min	t_{90} / min	CRI / min ⁻¹
Neat NR	3.3 ± 0.1	6.0 ± 0.3	8.4 ± 0.4	41.7
NR/neat silica	4.2 ± 0.4	10.2 ± 0.6	20.4 ± 0.3	9.8
NR/MPTMS-silica	5.4 ± 0.0	8.5 ± 0.0	14.3 ± 0.0	17.2
NR/MPS-silica	5.2 ± 0.1	6.2 ± 0.0	11.4 ± 0.3	19.2

^a $\Delta S = (M_H - M_L)$.

4. VULCANIZATION KINETICS

Vulcanization characteristics expressed as the difference of maximum and minimum torque values (ΔS), scorch time (t_{S2}), optimum cure time (t_{90}) for the neat NR and NR + silica composites is presented in Table II.

It is found that ΔS increases on loading with silica. NR composites containing neat silica exhibit higher ΔS values than neat NR—an effect that can be explained by silica–silica network formation.²⁶ It is worth noting that a reduction in silica–silica aggregation due to the presence of silane, leading to lower ΔS values than for NR composites containing neat silica was expected. However, contrary to the conventional wisdom, higher ΔS values for the NR composites containing silane modified silica—either MPTMS-silica or MPS-silica—are found. This effect may be attributed to stronger interactions between silane modified silica and rubber matrix or else to a higher degree of crosslinking compared to the NR composites containing the neat silica, leading to a more stiffness. Scorch time (t_{S2}) that is the time during which a rubber compound can be worked at a given temperature before curing begins, and optimum cure time (t_{90}) of the NR vulcanizates increase for the NR + silica composites. The adsorption of basic accelerator due to the presence of OH groups on the

surface of silica has apparently contributed to these longer times.^{6, 19, 20}

Vulcanization kinetics of rubber compounds can be investigated using several techniques such as DSC, moving die rheometry (MDR) and oscillating disc rheometry (ODR) under isothermal conditions. We have applied DSC with the dynamic multi-heating scan. The dynamic method provides kinetic parameters with good accuracy.^{25, 27} A basic concept of the dynamic multi-heating scan analysis is that the peak exotherm temperature T_p varies in a predictable manner with the heating rate β . An example of the dependence of T_p on the variation of β is shown as in Figure 3. According to the Kissinger analysis, the activation energy for vulcanization can be obtained from the maximum reaction rate where the exothermal peak appears under a constant heating rate:

$$E_a = -R \left[\frac{d(\ln(\beta/T_p^2))}{d(2/T_p)} \right] \quad (3)$$

Thus, the activation energy E_a can be obtained from the slope of the plot of $\ln(\beta g/T_p^2)$ as a function of $1/T_p$ without making specific assumptions on the nature of the conversion-dependence function.²⁰ The results are shown in Table III.

We see in Table III that E_a values increase by ≈ 66 , 26 and 48 kJ/mol by adding neat silica, MPTMS-silica and MPS-silica, respectively, to the NR matrix. Thus, the addition of any of our silicas inhibits the crosslinking reaction of the NR matrix. More energy is needed for curing NR + silica composites. However, E_a s of our nanocomposites with modified silica are lower E_a than that of NR + neat silica. Thus, modification of silica surfaces can improve the capability of vulcanizing NR containing silica

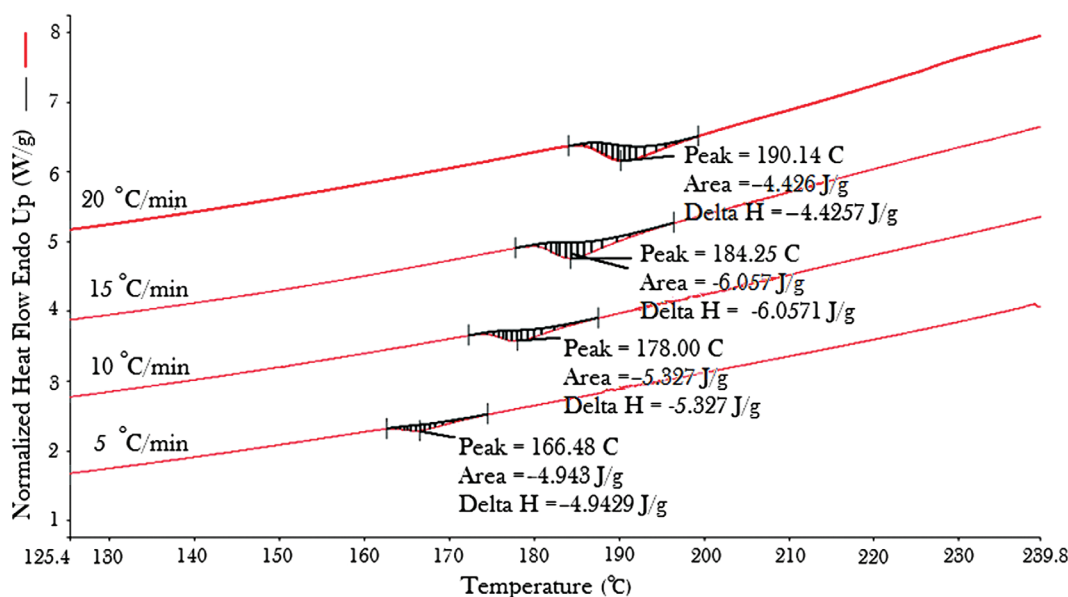


Fig. 3. DSC thermogram of the neat rubber at the heating rates of 5, 10, 15 and 20 °C/min.

Table III. Activation energy of the neat NR and nanocomposites.

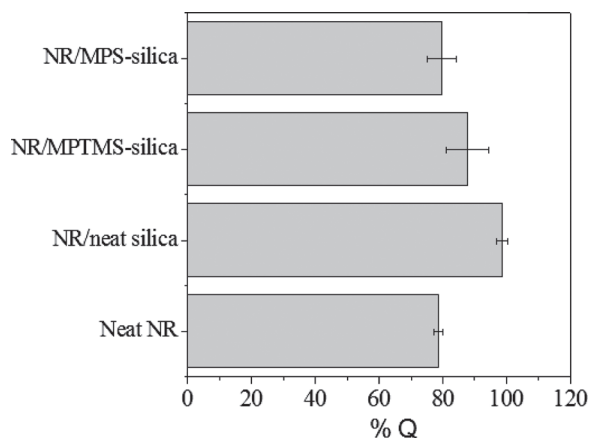
Sample	E_a /(kJ/mol)
Neat NR	87.3 ± 0.6
NR/neat silica	153.5 ± 5.8
NR/MPTMS-silica	113.6 ± 3.8
NR/MPS-silica	135.6 ± 3.4

filler. Our DSC results agree with those from vulcanization kinetics shown in Table II. The cure rate index (CRI) values defined by Eq. (1) of NR + surface-modified silica composites are approximately twice the value for NR + neat silica. We see in Table II that the neat silica containing system has the lowest CRI while the same system has in Table III the highest activation energy.

5. SWELLING PROPERTIES

The effect of the surface modification of silica on the crosslink density was determined from the swelling behavior of NR composites according to Eq. (2). During the swelling test, an uncrosslinked part of NR composites is presumed to be extracted by toluene; thus, what remains is the crosslinked constituent of the composites. Therefore, the percentage degree of swelling Q is inversely proportional to the degree of crosslinking. Figure 4 shows the percentage degree of swelling Q of the neat NR and of the nanocomposites. As can be seen, the Q values for all composites are higher than those of the neat NR. Further, the nanocomposites containing silane-modified silica show lower Q values than the NR containing neat silica. We find that the crosslink density of NR is enhanced by modification of the surface of silica.

We also see that the MPS containing nanocomposite undergoes swelling less than that containing MPTMS. When we look again at the chemical structures in Figure 1, we see that the MPS molecule is smaller. Longer chains of MPTMS make possible more extensive swelling.

**Fig. 4.** Degree of swelling Q of the neat NR and of the nanocomposites.

6. DYNAMIC MECHANICAL ANALYSIS (DMA)

The effect of surface-modified silica on dynamic mechanical behavior of NR was investigated. The storage modulus G' , the loss modulus G'' were determined as a function of temperature, providing also values of $\tan \delta$ since

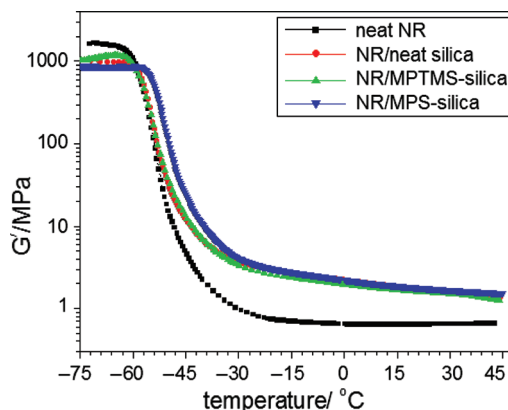
$$\tan \delta = G''/G' \quad (4)$$

We recall that the storage modulus reflects the recoverable (elastic, solidlike) energy in a deformed specimen while G'' represents the (liquidlike) energy lost by dissipation.

Figure 5 shows the storage modulus G' of our materials at the frequency of 1.0 Hz.

At low temperatures, that is in the glassy state, the storage modulus G' of the neat NR exhibits relatively high values due to inherent semi-crystalline characteristics.²⁸ Interestingly, the addition of silica, either untreated or treated one, causes a reduction in G' at the glassy range. This could be considered as contrary to expectations, namely we have a weakening effect instead of reinforcement. However, recall here the results reported in the preceding Sections. The presence of silica lowers the curing rate, causes an increase in the activation energy of the curing reaction, and increases the degree of swelling — and thus causes a lowering of the crosslink density and lower G' .

As discussed in Ref. [29], the midpoint of the fall of G' provides well the location of the glass transition temperature T_g . Above T_g the situation is inverted. Addition of silica causes an increase of G' ; now the reinforcement does its job. This applies to the descending parts of $G'(T)$ curves as well as to the subsequent rubbery plateau. We note that the modification of silica has a varying effect on the descending parts while the nearly horizontal rubbery plateau regions is nearly the same for all silica modifications—but always clearly above the curve for neat NR. We recall how the addition of nm size silica particles has increased the wear resistance of an epoxy.⁸ We also

**Fig. 5.** The storage modulus G' of the neat NR and the nanocomposites at 1.0 Hz versus temperature.

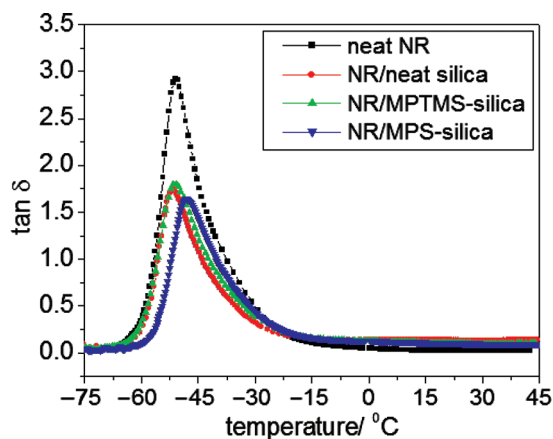


Fig. 6. $\tan\delta$ of the neat NR and NR/silica composites at 1.0 Hz.

recall how the addition of silica improves thermal stability of poly(methyl acrylate).³⁰

Figure 6 shows the loss factor $\tan\delta$ as a function of temperature for neat NR and our three nanocomposites at the frequency of 1.0 Hz. We recall that the brittleness of materials is defined in terms of the tensile elongation at break ε_b and also of $E'(1.0 \text{ Hz})$.³¹ We further recall that $\tan\delta$ is related to the penetration depth in scratch testing;³² at any load, that depth increases along with the $\tan\delta$ increase.

We see in Figure 6 lower intensities of relaxations in the glass transition region of our nanocomposites as compared to neat NR. Clearly the presence of silica in any form hinders the relaxation processes. We recall that silica particles hinder viscoelastic recovery in scratch healing in copolymers of butyl acrylate and methyl methacrylate.³³

A peak of $\tan\delta$ in the glass transition region can also be used for location of the glass transition temperature;²⁹ we recall that T_g always represents a temperature range and Figure 6 confirms this fact. There are slight modifications of T_g of NR by silicas, in fact in both directions. Lowering of T_g by unmodified silica and by silica modified by MPTMS can be explained by lower degrees of curing and thus enhancement of the chain mobility.

By contrast, T_g of the system containing MPS-silica is slightly higher. This can be explained by strong interactions of the filler with the NR matrix. We have noted in the previous section that the material containing MPTMS undergoes more extensive swelling because of longer chains. Now longer molecules of MPTMS move the glass transition region downwards—while shorter molecules of MPS do not have such an effect.

Mele et al.³⁴ detected a decrease in T_g of their styrene-butadiene rubber (SBR) reinforced with silane treated silica; they ascribed this response to an unspecified form of mechanical coupling between the rigid filler, boundary layer and bulk rubber. Giunta³⁵ and Arrighi et al.³⁶ also found similar reductions in T_g . Giunta additionally postulated the existence of a broadened relaxation spectrum

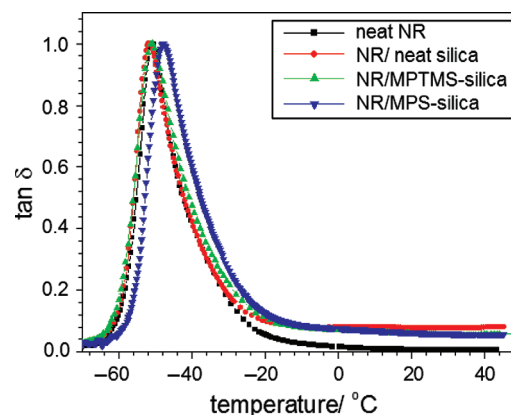


Fig. 7. Normalized $\tan\delta$ as a function of temperature of the neat NR and nanocomposites at 1.0 Hz.

of the constrained phase while such a spectrum was not found in Arrighi's system.

To evaluate the hypothesis of spectrum broadening, we have plotted the normalized $\tan\delta$ curves for our materials in Figure 7. The widths at half peak maxima were determined. No broadening compared to the neat NR is observed.

Relaxation peaks are known to shift to higher temperatures when the frequency increases. One uses an Arrhenius type equation:

$$f = f_0 \exp(-E_{ar}/RT) \quad (5)$$

where f_0 is a constant, f is the test frequency, R is the gas constant and E_{ar} is the activation energy for relaxation process (different from E_a discussed above). The activation energy can be calculated directly from the $-R \times$ slope of the plot of $\ln f$ as a function of $1000/T$ as shown in Figure 8. The activation energies E_{ar} so calculated are presented in Table IV.

E_{ar} for the relaxation process is defined as the energy for molecules to move from one equilibrium position to another such position.³⁷ It is found from Table IV that E_{ar}

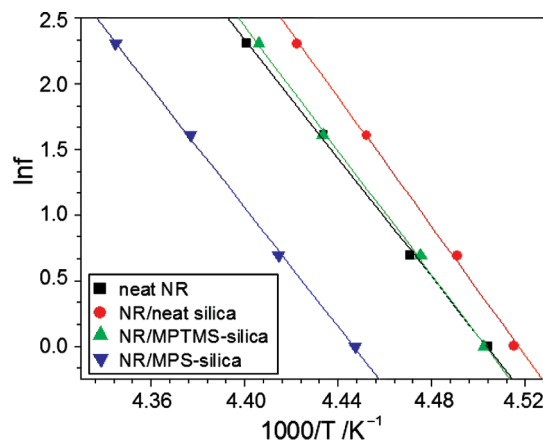


Fig. 8. $\ln f$ as a function of $1000/T$.

Table IV. Activation energy of the relaxation process.

Sample	E_{ar} /(kJ/mol)
Neat NR	187.3 ± 4.9
NR/neat silica	204.3 ± 6.3
NR/MPTMS-silica	196.4 ± 4.3
NR/MPS-silica	188.8 ± 3.6

of the neat NR is lower than those for the nanocomposites. Apparently the addition of silicas to NR reduces the chain mobility. The effect is very small for the composite containing MPS-silica in which, as discussed above, stronger matrix + filler interactions take place.

Within less than a decade, nanoscience and nanotechnology have become integral elements of education at a number of universities worldwide.^{38–43} Reinforcement of natural rubber by ceramic particles seems to have some instructional advantages for presenting nanoscience and nanotechnology by a simple example.

References and Notes

- M. D. Frogley, D. Ravich, and H. D. Wagner, *Comp. Sci. Technol.* 63, 1647 (2003).
- A. Bandyopadhyay, M. De Sarkar, and A. K. Bhowmick, *J. Mater. Sci.* 40, 53 (2005).
- A. Bandyopadhyay, M. De Sarkar, and A. K. Bhowmick, *Rubber Chem. & Technol.* 78, 806 (2005).
- A. P. Meera, S. Saidi, Y. Grohens, and S. Thomas, *J. Phys. Chem. C* 113, 17997 (2009).
- Y. Urushihara, L. Li, J. Matsui, and T. Nishino, *Composites A* 40, 232 (2009).
- P. Sae-oui, C. Sirisinha, U. Thepsuwan, and K. Hatthapanit, *Eur. Polymer J.* 43, 185 (2007).
- L. Mathew and S. K. Narayanankutty, *Polymer-Plastics Tech. & Eng.* 48, 75 (2009).
- W. Brostow, W. Chonkaew, T. Datashvili, and K. P. Menard, *J. Nanosci. Nanotechnol.* 8, 1916 (2008).
- F. Huguenin, M. Ferreira, V. Zucolotto, F. J. Nart, M. R. Torresi, and O. N. Oliveira, Jr., *Chem. Mater.* 16, 2293 (2004).
- D. S. dos Santos, Jr., P. J. G. Goulet, N. P. W. Pieczonka, O. N. Oliveira, Jr., and R. F. Aroca, *Langmuir* 20, 10273 (2004).
- R. F. Aroca, D. S. dos Santos, Jr., R. A. Alvarez-Puebla, and O. N. Oliveira, Jr., *Anal. Chem.* 77, 378 (2005).
- W. Brostow, B. P. Gorman, and O. Olea-Mejia, *Mater. Lett.* 61, 1333 (2007).
- W. Brostow, A. Buchman, E. Buchman, and O. Olea-Mejia, *Polymer Eng. & Sci.* 48, 1977 (2008).
- O. Olea-Mejia, W. Brostow, and E. Buchman, *J. Nanosci. Nanotechnol.* 10, in press (2010).
- Z. Roslaniec, G. Broza, and K. Schulte, *Compos. Interfaces* 10, 95 (2003).
- A. Nogales, G. Broza, Z. Roslaniec, K. Schulte, I. Sics, B. S. Hsiao, A. Sanz, M. C. Garcia-Gutierrez, D. R. Rueda, C. Domingo, and T. A. Ezquerro, *Macromolecules* 37, 7669 (2004).
- A. K. Kota, B. H. Cipriano, D. Powell, S. R. Raghavan, and H. A. Bruck, *Nanotech.* 18, 505705 (2007).
- H. Yan, K. Sun, Y. Zhang, and Y. Zhang, *Polym. Test.* 24, 32 (2005).
- N. Rattanasom, T. Saowapark, and C. Deeprasertkul, *Polym. Test.* 26, 369 (2007).
- A. M. Shanmugaraj, J. H. Bae, K. Y. Lee, W. H. Noh, S. H. Lee, and S. H. Ryu, *Comp. Sci. Technol.* 67, 1813 (2007).
- A. Ansarifard, A. Azhar, N. Ibrahim, S. F. Shiah, and J. M. D. Lawton, *Inter. J. Adhes. Adhes.* 25, 77 (2005).
- S. J. Park and K. S. Cho, *J. Colloid Interface Sci.* 267, 86 (2003).
- N. Suzuki, M. Ito, and F. Yatsuyanagi, *Polymer* 46, 193 (2005).
- J. W. ten Brinke, S. C. Debnath, L. A. E. M. Reuvekamp, and J. W. M. Noordermeer, *Comp. Sci. Technol.* 63, 1165 (2003).
- K. P. Menard, Performance of Plastics, edited by W. Brostow, Hanser, Munich–Cincinnati (2000), Chap. 8.
- C. Gauthier, E. Reynaud, R. Vassoille, and L. Ladouce-Stelandre, *Polymer* 45, 2761 (2004).
- R. B. Prime, Thermal Characterization of Polymeric Materials, edited by E. A. Turi, Academic Press, New York (1981), p. 972.
- G. Sui, W. H. Zhong, X. P. Yang, and Y. H. Yu, *Mater. Sci. Eng. A* 485, 524 (2008).
- W. Brostow, S. Deshpande, D. Pietkiewicz, and S. R. Wisner, *e-Polymers no.* 109 (2009).
- W. Brostow, T. Datashvili, and K. P. Hackenberg, *e-Polymers no.* 054 (2008).
- W. Brostow, H. E. H. Lobland, and M. Narkis, *J. Mater. Res.* 21, 2422 (2006).
- W. Brostow, W. Chonkaew, and K. P. Menard, *Mater. Res. Innovat.* 10, 389 (2006).
- A. F. Vargas, W. Brostow, H. E. H. Lobland, B. L. Lopez, and O. Olea-Mejia, *J. Nanosci. Nanotechnol.* 9, 6661 (2009).
- P. Mélé, S. Marceau, D. Brown, Y. de Puydt, and N. D. Albérola, *Polymer* 43, 5577 (2002).
- R. Giunta, Ph.D. Thesis, Virginia Polytechnic Institute and State University (1999).
- V. Arrighi, I. J. McEwen, H. Qian, and M. B. S. Prieto, *Polymer* 44, 6259 (2003).
- J. P. Pascault, H. Sautereau, J. Verdu, and R. J. J. Williams, Thermosetting Polymers, Marcel Dekker, New York (2002), p. 477.
- K. Cowan and Y. Gogotsi, *J. Mater. Ed.* 26, 147 (2004).
- K. J. Pawlowski, C. P. Barnes, E. D. Boland, G. E. Wnek, and G. L. Bowlin, *J. Mater. Ed.* 26, 195 (2004).
- D. Hammer and D. Srikantaiah, *J. Mater. Ed.* 26, 245 (2004).
- M. Meyyappan, *J. Mater. Ed.* 26, 313 (2004).
- L. C. Klein, *J. Mater. Ed.* 28, 7 (2006).
- D. -B. Shieh, C. -S. Yeh, W. -C. Chang, and Y. Tzeng, *J. Mater. Ed.* 29, 107 (2007).

Received: 24 November 2009. Accepted: 18 April 2010.